Capillary zone electrophoresis with indirect UV detection applying a UV-absorbing counter ion

J. Collet, P. Gareil*

Laboratoire d'Electrochimie et de Chimie Analytique (URA CNRS 216), Ecole Nationale Supérieure de Chimie de Paris, 11 rue Pierre et Marie Curie, 75231 Paris Cedex 05, France

Abstract

The method of choice for the determination of non-UV-absorbing ions in capillary zone electrophoresis (CZE) usually consists in applying indirect UV detection with a non-UV-absorbing counter ion and a UV-absorbing co-ion (chromophore). Nevertheless, the use of chromogenic species with a sign of charge opposite to that of the analyte has recently been mentioned with regard to its principle but has not yet given rise to practical development. In this paper, the indirect UV detection of cations using anionic chromophores (benzoate, anisate) and cationic buffers (Tris, ethanolamine) is described. Based on the use of Kohlrausch's regulation function, a new equation for the response factor (k_r) has been derived. Depending on the absolute mobility of the analyte ion relative to that of the co-ion, both negative and positive peaks can be observed. The separation of some alkali metal ions and quaternary ammonium ions was used to confirm the dependence of k_r on the absolute mobilities of the three components of the system (analyte ion, co-ion and counter ion). In addition, the peak shape of a weak analyte (ammonium ion) is also presented as a function of pH. From these results, it can be shown that using the proper pH, a higher efficiency can be reached by matching the effective mobility of the UV-transparent co-ion more closely to those of the analyte ions.

1. Introduction

In 1989, Foret et al. [1] provided a set of rules towards method development for the indirect UV detection of non-absorbing ions using charge displacement of an absorbing co-ion as a principal constituent of the background electrolyte. Since then, this mode of detection has become very popular in CZE, especially for the determination of inorganic anions and cations [2,3]. Relevant additional theoretical aspects were also published [4–7]. However, Foret et al. [1] also recognized the feasibility of detecting cations (K^+, Li^+) with an anionic chromophore (sor-

bate), but little attention has been paid to the development of practical applications. Nevertheless, the mathematical model, using the eigenvector approach, that was formulated by Poppe [7] for the simulation of indirect absorbance electropherograms was of sufficiently general scope to account for both counter ionic and co-ionic chromophores. While this work was under way, Beckers [8], assuming only the presence of fully ionized monovalent ionic components, shed light on the different approaches for UV detection in CZE: the detection of positive and negative peaks (dips) was discussed with respect to the UV absorbance or transparency of the analyte and of the electrolyte co-ion and counter ion. The appearance of system peaks

---

* Corresponding author.

occurring with electrolytes containing two co-ions was also displayed.

In this paper, we report similar observations for the indirect UV detection of strong (alkali metal, quaternary ammonium ions) or weak (NH_4^+) analytes applying a UV-transparent co-ion and a UV-absorbing counter ion. Both theoretical and experimental aspects of this original mode of detection are presented using response factor calculations, derived from the well known Kohlrausch's regulation function (KRF) [9]. Relative merits and drawbacks of the KRF approach are exemplified for the description of some indirect UV detection systems.

2. Theoretical

2.1. Strong electrolytes

Starting with Kohlrausch's regulation function, it holds for strong and multivalent electrolytes [10] that

$$\sum_i \frac{Z_i C_i}{m_i} = \omega \tag{1}$$

where Z_i is the absolute value of the charge of component i, C_i its concentration and m_i the absolute value of its mobility ($m_i \geq 0$); ω states the numerical value of KRF that is supposed to be locally invariant with time. For a background electrolyte AB composed of a co-ion A and a counter ion B applied to the electrophoresis of a sample ion i, it follows that

$$\frac{Z_A C_A^E}{m_A} + \frac{Z_B C_B^E}{m_B} = \frac{Z_A C_A^S}{m_A} + \frac{Z_B C_B^S}{m_B} + \frac{Z_i C_i^S}{m_i} \tag{2}$$

The superscripts E and S refer to the carrier electrolyte AB zone and the sample zone, respectively. In Eq. 2 we assume that the contributions from H^+ and OH^- to KRF are negligible at an intermediate pH. We also assume that the mobilities m_A, m_B and m_i are constant regardless of the zone E or S.

Electroneutrality demands that

$$Z_A C_A^E = Z_B C_B^E \tag{3}$$

and

$$Z_A C_A^S + Z_i C_i^S = Z_B C_B^S \tag{4}$$

Substituting Eqs. 3 and 4 into Eq 2 results in

$$C_B^E = C_B^S - k_i \cdot \frac{Z_i}{Z_B} \cdot C_i^S \tag{5}$$

with

$$k_i = \frac{m_B}{m_A + m_B} \left(1 - \frac{m_A}{m_i}\right) \tag{6}$$

In the case of a UV-transparent solute i, a UV-transparent co-ion A and a UV-absorbing counter ion B, the application of Beer's law leads to the following expressions for the absorbance of the carrier electrolyte, A^E:

$$A^E = \varepsilon_B l C_B^E = \varepsilon_B l C_B^S - \varepsilon_B l k_i \cdot \frac{Z_i}{Z_B} \cdot C_i^S \tag{7}$$

and for the absorbance of the sample zone, A^S:

$$A^S = \varepsilon_B l C_B^S \tag{8}$$

Combination of Eqs. 7 and 8 yields

$$\Delta A = A^S - A^E = \varepsilon_B l k_i \cdot \frac{Z_i}{Z_B} \cdot C_i^S \tag{9}$$

where ε_B is the molar absorptivity of component B (chromophore) and l the optical path length. It may be seen from Eq. 9 that k_i represents the response factor of the sample ion i. Depending on the sign of k_i, both negative peaks (for $m_i < m_A$) and positive peaks (for $m_i > m_A$) can be observed in the electropherogram. Finally, $m_i = m_A$ leads to $k_i = 0$ (no peak). This model was previously described by Beckers [8] for monovalent ions. In the present work, as far as multivalent ions are considered, it ensues that (i) ΔA is proportional to Z_i, (ii) ΔA is in inverse proportion to Z_B and (iii) ΔA is independent of Z_A.

By analogy with Ackermans' treatment [4], it can be shown that the measured peak area of a

solute ion i (A_i) is directly proportional to the concentration c_i^S, the charge Z_i, the migration time t_i and the response factor k_i. In other words, it can be expected that the relationship between $A_i/C_iZ_it_i$ and k_i is linear, passing through the origin.

2.2. Weak electrolytes

The question of whether KRF can be applied to weak electrolytes is of great relevance for a correct interpretation of indirect UV detection profiles. It has already been pointed out by Poppe [7] that KRF is not suitable for components in acid–base equilibrium, and in cases where pH variations between analyte and electrolyte zones may occur. If pH cannot be carefully controlled during the separation process, then the apparent charges of weak constituents are no longer constant in Eq. (2). As a consequence, the use of KRF should be theoretically restricted to strong electrolytes. Unfortunately, this case does not correspond to the current practical situation, where weak analytes dictate the choice of weak electrolyte components for adequate buffering capacity. In the present investigation, we examined the relative merits and limitations of the KRF approach for the modelling of some indirect UV detection systems.

3. Experimental

Measurements were carried out with an Applied Biosystems (Santa Clara, CA, USA) Model 270A capillary electrophoresis system equipped with a 72 cm long (50 cm to the detector cell) × 50 μm I.D. fused-silica capillary column. All experiments were performed at 30°C, at constant voltage, under normal polarity (anode at the inlet). Samples were introduced hydrodynamically by application of vacuum. Data were recorded on a Spectra-Physics (San Jose, CA, USA) Model 4400 integrator. Chemicals used as electrolyte components and test solutes were of analytical-reagent grade.

4. Results and discussion

4.1. Strong analytes

In order to verify the relationship between the response factor k_i and the mobilities of the three components of the system (solute ion i, co-ion A and counter ion B) (Eq. 6), the separation of seven fully ionized cations [potassium, barium, sodium, lithium, tetraethylammonium (TEA), tetrapropylammonium (TPA) and tetrabutylammonium (TBA)] was achieved employing 15 mM potassium–benzoate buffer, 15 mM sodium–benzoate buffer or 10 mM Tris–anisate buffer (displayed in Fig. 1 as systems 1, 2 and 3, respectively). As shown in electropherogram 1.1, all components are detected as dips, because $m_i < m_A$ for all solutes i (see Tables 1 and 2). The potassium peak is absent in system 1 ($m_i = m_A$). In system 2, only four solute ions give negative dips (lithium, TEA, TPA, TBA), whereas positive peaks are obtained for those (potassium, barium) satisfying the condition $m_i > m_A$. In addition, and as a consequence of electromigration dispersion, fronting or tailing peaks are observed for solutes having a mobility higher or lower (respectively) than the mobility of the co-ion, so that peaks at a time change their polarity and asymmetry in accordance with m_i with respect to m_A values. Then it is readily apparent that the major limitation of this detection mode for quantitative analysis lies in the fact that the maximum efficiency is obtained when the response factor is zero.

The results presented in systems 1 and 2, in which all solutes and electrolyte co-ions are strong electrolytes, are in good agreement with the previous treatment of Beckers [8]. More interesting, however, is the description of system 3 (10 mM p-anisic acid adjusted to pH 8.24 by adding Tris). In contrast to systems 1 and 2, where the buffering capacity was controlled by the counter ion, the pH is now governed by the co-ion (Tris). Since the pH chosen is close to the pK_a of Tris, it follows that the effective mobility of Tris is about half of its absolute mobility, ca. $15.2 \cdot 10^{-5}$ cm^2 V^{-1} s^{-1}. This calculation includes corrections for temperature and ionic strength
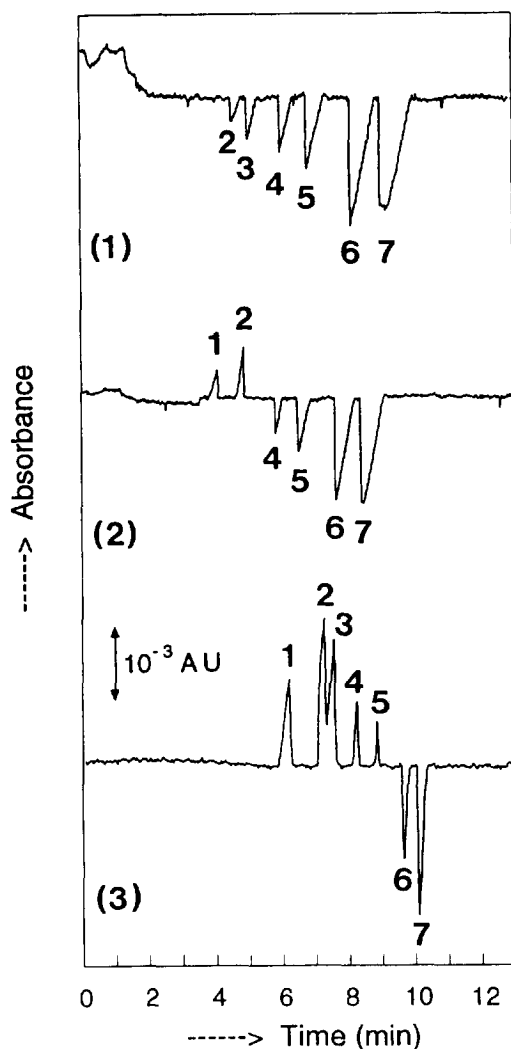
Fig. 1. Zone electrophoretic separations of seven fully ionized UV-transparent cations applying indirect UV detection with a chromogenic counter ion. Fused-silica capillary, 72 cm × 50 μm I.D. (effective length 50 cm). Temperature, 30°C. Peaks: 1 = potassium; 2 = barium; 3 = sodium; 4 = lithium; 5 = tetraethylammonium (TEA); 6 = tetrapropylammonium (TPA); 7 = tetrabutylammonium (TBA). Pressure injection for 5 s. System 1: carrier electrolyte, 15 mM benzoic acid adjusted to pH 4.60 by adding KOH. Sample: aqueous solution of 2 mM of each ion, except for sodium (4 mM). Wavelength, 254 nm. Applied voltage, +15 kV. System 2: 15 mM benzoic acid adjusted to pH 4.60 by adding NaOH. Other conditions as in system 1. System 3: 10 mM p-anisic acid adjusted to pH 8.24 by adding tris [tris(hydroxymethyl) aminomethane]. Sample: aqueous solution of 0.5 mM of each ion, except for sodium (1 mM). Wavelength, 270 nm. Applied voltage, +7.5 kV. See text for further explanations.

Table 1
Electrophoretic mobilities (10^{-5} cm^2 V^{-1} s^{-1}) of the test compounds as determined in this work using electrolyte systems 1, 2 and 3 (see Fig. 1)

Solute ion	System 1	System 2	System 3
K$^+$	–	71.7 (0.5)	71.0 (0.5)
Ba^{2+}	61.8 (0.5)	55.7 (0.2)	52.1 (0.1)
Na$^+$	51.0 (0.3)	–	47.8 (0.2)
Li$^+$	41.1 (0.3)	40.4 (0.2)	38.5 (0.1)
TEA$^+$	33.3 (0.2)	33.0 (0.2)	31.6 (0.1)
TPA$^+$	24.1 (0.2)	24.1 (0.1)	24.0 (0.1)
TBA$^+$	19.1 (0.2)	19.3 (0.1)	20.0 (0.1)

Temperature: 30°C. Average values were calculated from four successive experiments. Standard deviations are given in parentheses.

(Table 2). On the other hand, it appears from Fig. 1 (3) that the inversion point of the signal polarity is located between the TEA peak ($m_i = 31.6 \cdot 10^{-5}$ cm^2 V^{-1} s^{-1}) and the TPA dip ($m_i = 24.0 \cdot 10^{-5}$ cm^2 V^{-1} s^{-1}) (Table 1), suggesting that the condition for signal polarity inversion is still related to the absolute mobility of the co-ion, rather than to its effective mobility.

This observation also led us to consider that the expression for the response factor k_i (Eq. 6) could still be valid introducing the absolute mobility of co-ion A, m_A^0. In effect, if the ratio $A_i/c_i z_i t_i$, calculated from experimentally measured (t_i, A_i) and known (c_i, z_i) values, is plotted against response factors k_i (Fig. 2), calculated as stated above, the expected linear fitting is obtained for systems 1, 2 and 3. Noteworthy is the correct prediction for the divalent barium peak ($Z_i = 2$). More important, the linearity of these plots and the zero intercepts are fairly good in comparison with the results obtained by Ackermans et al. [4] with a UV-absorbing co-ion. This can be explained by the fact that in the present system where a UV-absorbing counter ion is applied, a larger range of response factors can be explored ($0 \le k_i \le 0.8$ in system 1 and $-0.7 \le k_i \le 0.1$ in system 2) compared with that exploited in Ref. [4] ($0.7 \le k_i \le 1.1$ in the best case). A comparison of these response factor values also suggests that the best sensitivity is generally obtained when a UV-absorbing co-ion

Table 2
Estimated absolute mobilities (10^{-5} cm^2 V^{-1} s^{-1}) derived from the literature, assuming an average correction factor of 2%/°C and using the Debye–Hückel equation for the correction of ionic strength

Ion	From literature (25°C, infinite dilution)	After correction for temperature (30°C) and ionic strength (μ)
Tris	29.5 [11]	30.5 ($\mu = 10$ mM)
Ethanolamine	44.3 [11]	44.5 ($\mu = 10$ mM)
NH_4^+	76.1 [12]	78.6 ($\mu = 10$ mM)
Anisate	30.0 [13]	28.8 ($\mu = 10$ mM)
Benzoate	33.6 [11]	31.6 ($\mu = 15$ mM)

is applied (the usual case for indirect absorbance detection), because of the higher values of k_i that can be reached in this situation.

The slopes of the plots of $A_i/c_i z_i t_i$ versus k_i are given in Fig. 2. In agreement with Eq. 9 showing that ΔA is proportional to ε_B, the slopes obtained with the potassium–benzoate and sodium–benzoate carrier electrolytes are nearly identical (53.6 and 49.3). Using the Tris–anisate system, the slope is about four times increased because of the higher molar absorptivity of anisate. From the preceding results, it can be inferred that predictions from KRF still remains valid with strong analytes and electrolytes containing either weak counter or co-ions.

4.2. Weak analytes

In the theoretical section, we discussed the problem of whether KRF is applicable to cases with acid–base equilibria involving both the sample and the carrier electrolyte constituents. Fig. 3 shows an electropherogram of four strong monovalent cations and weakly acidic ammonium ion obtained by using 10 mM p-anisic acid adjusted to pH 9.90 with ethanolamine. Two important features can be emphasized from this separation: first, NH_4^+ gives a positive peak, as if its response factor were controlled by absolute mobilities. In fact, the absolute mobility (m_i^0) of NH_4^+ in the present conditions was estimated from the experiments to be $78.6 \cdot 10^{-5}$ cm^2 V^{-1} s^{-1} and the absolute mobility of ethanolamine (m_A^0) (fully protonated form) is $44.5 \cdot 10^{-5}$ cm^2

V^{-1} s^{-1} (Table 2). Hence the condition $m_i^0 > m_A^0$ still results in a positive response factor for NH_4^+. Second, the detection of NH_4^+ is accompanied by a high efficiency (about 270 000 theoretical plates in Fig. 3), giving rise to some questions.

In order to clarify this crucial point, a set of additional experiments was carried out at different pH values ranging from 8.51 to 10.20 using 10 mM ethanolamine–anisate as background electrolyte and NH_4^+ as a test solute. The influence of pH on the ammonium peak shape is shown in Fig. 4 and the corresponding measured efficiencies are plotted in Fig. 5. These experimental findings can be better understood in comparing the effective mobility values of NH_4^+ and ethanolamine. Based on absolute mobility (Table 2) and acidity constant estimations accounting for the actual values of temperature and ionic strength, it turns out that the calculated effective mobility of NH_4^+ is higher than that of ethanolamine until pH 10.0, beyond which the two values remain almost equal (Fig. 6). It can be seen that the optimum efficiency for NH_4^+ is reached when the effective mobility of the ammonium ion matches the effective mobility of ethanolamine. Curiously, this behaviour is not observed for TBA and TPA, which exhibited strong tailings in Figs. 1(3) and 3, although the basic theory predicts that fronting peaks should be expected in a situation for which the effective mobility of the analyte ion is superior to that of the background electrolyte co-ion. In our opinion, this apparent contradiction lays the stress on the limited ability of Kohlrausch's regulation function to deal with such complicated systems.
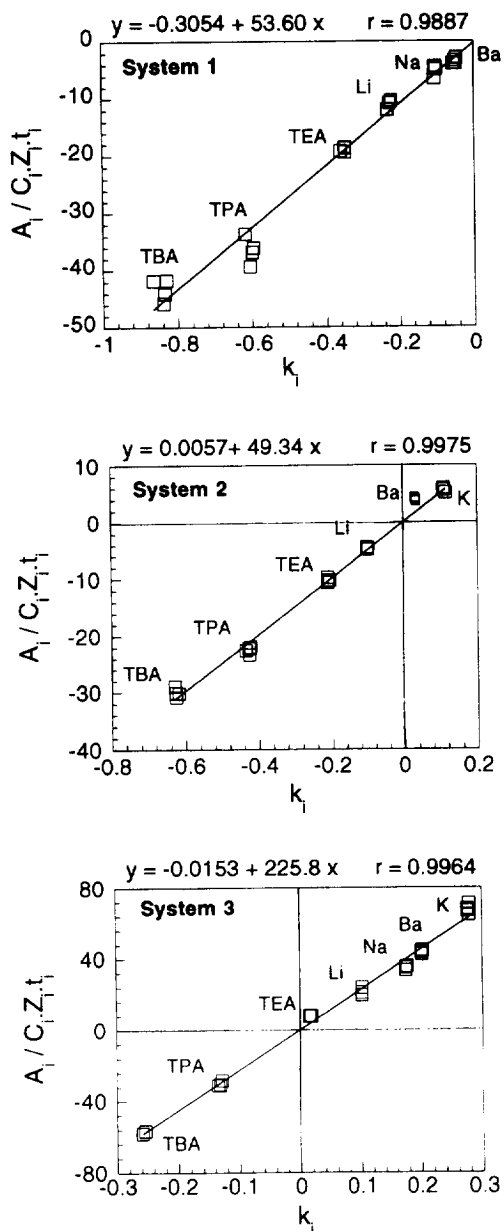
$y = -0.3054 + 53.60\,x \quad r = 0.9887$

System 1

$A_i / C_i Z_i t_i$

k_i

$y = 0.0057 + 49.34\,x \quad r = 0.9975$

System 2

$A_i / C_i Z_i t_i$

k_i

$y = -0.0153 + 225.8\,x \quad r = 0.9964$

System 3

$A_i / C_i Z_i t_i$

k_i

Fig. 2. Plots of $A_i/c_i z_i t_i$ (arbitrary units) versus k_i associated with the experiments illustrated in Fig. 1. t_i, A_i, migration times and peak areas, respectively, measured experimentally; c_i, z_i, analyte concentrations and charges, respectively (known values); k_i, response factor calculated according to Eq. 6 using absolute values of absolute mobilities from this work (Table 1) or the literature (Table 2). System 1, $m_A^0 = 71.7$ and $m_B^0 = 31.6$; system 2, $m_A^0 = 51.0$ and $m_B^0 = 31.6$; system 3, $m_A^0 = 30.5$ and $m_B^0 = 28.8$ (all values in 10^{-5} cm^2 V^{-1} s^{-1}). For solute ions, $Z_i = 1$ except for barium ($Z_i = 2$). For the chromophores, $Z_B = 1$ in all cases. Data were collected from four successive injections.
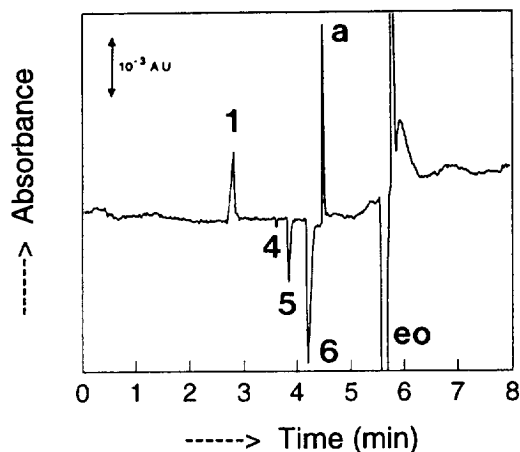

Fig. 3. Electropherogram of a mixture of potassium (1), lithium (4), tetraethylammonium (5), tetrapropylammonium (6) and ammonium (a) ions (0.5 mM each, pressure injection time 5 s) in the indirect UV absorption mode. Carrier electrolyte, 10 mM p-anisic acid adjusted to pH 9.90 by adding ethanolamine. Wavelength, 270 nm. Applied voltage, +15 kV. eo, signal produced by the electroosmotic flow.

5. Conclusion

This work was undertaken in order to provide further insight into the feasibility of detecting cationic solutes with an anionic chromophore. This alternative mode of indirect UV detection permits the simultaneous detection of cations and anions during a single run. It also allows a larger choice of non-UV-absorbing co-ions in comparison with that otherwise afforded by the limited list of chromophores suitable for indirect UV detection in CZE.

Supplementing the recent results published by Beckers [8], some important features were highlighted for weak electrolytes in this work. First, it can be recognized that the signal polarity is governed by an absolute mobility difference between the analyte ion and the co-ion, whereas a direct and intuitive viewpoint would have considered an effective mobility difference. Then, in agreement with the general concept of electromigration dispersion, we have experimentally demonstrated that the peak shape of a weak analyte is dependent on the effective mobility of the analyte ion relative to that of the co-ion. Taking advantage of this observation, sensitivity
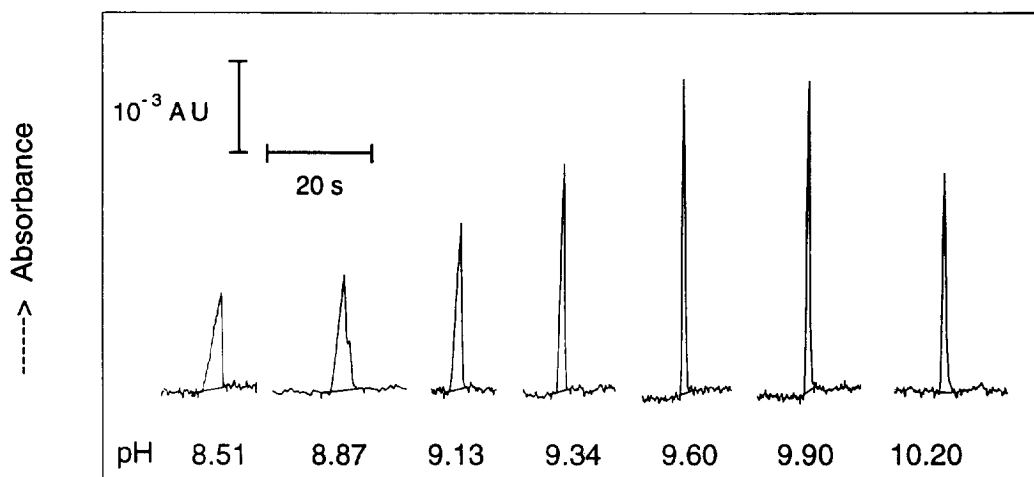
Fig. 4. Influence of pH on ammonium peak shape using 10 m*M* ethanolamine–anisate carrier electrolyte. Applied voltage, +30 kV. Detector rise time, 0.1 s. Other experimental conditions as in Fig. 3.

(related to peak efficiency) can be further improved by a proper choice of pH or employing complexing agents in order to minimize electromigration dispersion [15–17]. For example, 270 000 theoretical plates were reached for ammonium ion under the conditions described.

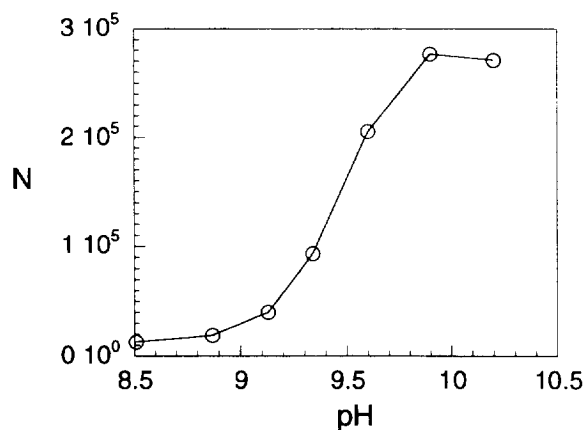Finally, quantitative aspects of indirect UV detection were also displayed using response

factor (k_i) calculations. As pointed out by Ackermans et al. [4], the relationship defined for k_i could be successfully applied to the development of universal calibration procedures for indirect UV detection in CZE, whatever chromogenic

Fig. 5. Number of theoretical plates (*N*) for the ammonium peak as a function of pH. Conditions as in Fig. 4. *N* was determined from the usual relationship $N = 5.54(t_m/\omega)^2$, where t_m is the migration time and ω the peak width at half-height. Average values of *N* were calculated from three successive experiments.
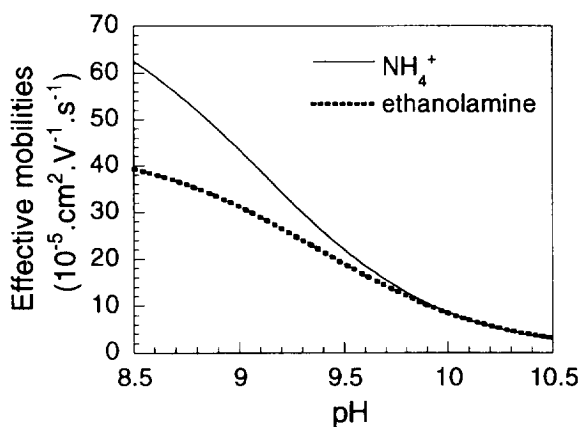

Fig. 6. Theoretical variations of the effective mobilities of ammonium and ethanolamine ions as a function of pH, accounting for an ionic strength of 10 m*M* and a temperature of 30°C. The p*K*$_a$ and m^0 values retained were as follows: for NH_4^+, p*K*$_a$ = 9.09 (from Ref. [14]) and $m_i^0 = 78.6 \cdot 10^{-5}$ cm^2 V^{-1} s^{-1} (from Table 2); for ethanolamine, p*K*$_a$ = 9.37 (from Ref. [14], assuming a correction for temperature of about -0.03 p*K*$_a$ unit/°C) and $m_A^0 = 44.5 \cdot 10^{-5}$ cm^2 V^{-1} s^{-1} (from Table 2). Considering weak bases, effective mobilities are defined as $m = m^0/(1 + 10^{pH - pK_a})$.

species plays the role of co-ion or of counter ion. This aspect is under investigation.

References

[1] F.Foret, S. Fanali, L. Ossicini and P. Bocek, J. Chromatogr., 470 (1989) 299.

[2] F. Foret, S. Fanali, A. Nardi and P. Bocek, Electrophoresis, 11 (1990) 780.

[3] J. Romano, P. Jandik, W.R. Jones and P.E. Jackson, J. Chromatogr., 546 (1991) 411.

[4] M.T. Ackermans, F.M. Everaerts and J.L. Beckers, J. Chromatogr., 549 (1991) 345.

[5] M.W.F. Nielen, J. Chromatogr., 588 (1991) 321.

[6] T. Wang and R.A. Hartwick, J. Chromatogr., 607 (1992) 119.

[7] H. Poppe, Anal. Chem., 64 (1992) 1908.

[8] J.L. Beckers, J. Chromatogr. A, 679 (1994) 153.

[9] F. Kohlrausch, Ann. Phys. (Leipzig), 62 (1897) 209.

[10] S. Hjertén, L.-G. Öfverstedt and G. Johansson, J. Chromatogr., 194 (1980) 1.

[11] T. Hirokawa, M. Nishino, N. Aoki, Y. Kiso, Y. Sawamoto, T. Yagi, J.I. Akiyama, J. Chromatogr., 271 (1983) D1.

[12] P. Bocek, M. Deml, P. Gebauer and V. Dolnik, in Radola (Editor) Analytical Isotachophoresis (Electrophoresis Library, Vol. 1), VCH, Weinheim, 1988.

[13] R.C. Weast (Editor), Handbook of Chemistry and Physics, CRC Press, Boca Raton, FL, 1988.

[14] D.D. Perrin, Dissociation Constants of Organic Bases in Aqueous Solutions, Butterworths, London, 1972.

[15] A. Weston, P.R. Brown, P. Jandik, W.R. Jones and A.L. Heckenberg, J. Chromatogr., 593 (1992) 289.

[16] G.W. Tindall, D.R. Wilder and R.L. Perry, J. Chromatogr., 641 (1993) 163.

[17] T.-I. Lin, Y.-H. Lee and Y.-C. Chen, J. Chromatogr. A, 654 (1993) 167.